

Article

Heat Treatment of Pine Wood: Possible Effect of Impregnation with Silver Nanosuspension

Hamid R. Taghiyari ^{1,*}, Siavash Bayani ², Holger Militz ³ and Antonios N. Papadopoulos ^{4,*}

¹ Department of Wood Science and Technology, Faculty of Materials Engineering & New Technologies, Shahid Rajaei Teacher Training University, Tehran 1678815811, Iran

² Department of Wood and Paper Science and Technology, College of Agriculture and Natural Resources, Science and Research Branch, Islamic Azad University, Tehran 22970021, Iran; siavash.bayani@yahoo.com

³ Burckhardt-Institute, Wood Biology and Wood Products, Georg-August-University Göttingen, 37077 Göttingen, Germany; hmilitz@gwdg.de

⁴ Laboratory of Wood Chemistry and Technology, Department of Forestry and Natural Environment, International Hellenic University, GR-661 00 Drama, Greece

* Correspondence: htaghiyari@sru.ac.ir (H.R.T.); antpap@for.ihu.gr (A.N.P.)

Received: 26 February 2020; Accepted: 16 April 2020; Published: 20 April 2020



Abstract: The scope of the present work was to study the effects of heat treatment (at different mild temperatures) on the physicochemical properties of pine wood, and to find out if impregnation with nanosilver may have any potential influence on the impact of heat treatment. Impregnation of wood with a 400-ppm silver nanosuspension was carried out under an initial vacuum pressure of 0.07 MPa, followed by a pressure of 0.25 MPa for thirty minutes, before heat treatment. Heat treatment was carried out under hot air at three relatively mild temperatures, 145, 165, and 185 °C. Results showed improvement of some properties in heat-treated wood at 145 °C. This was indicative of the improving impact caused by hornification and irreversible hydrogen bonding in the course of water movements due to heat treatment; significant fluctuations in the intensities of FTIR spectra bands at 1750–1500 cm⁻¹ were corroborating evidence of chemical alterations in hemicellulose polymer. The high mass loss at temperature 185 °C, and the extreme thermal degradation thereof, overcame the improving effects of hornification and formation of irreversible hydrogen bonds, consequently mechanical properties decreased significantly. Interaction of different elements involved made it hard to predict properties in specimens modified at 165 °C. Impregnation of specimens with nanosilver suspension resulted in significant increase of mass loss in specimens heat-treated at 185 °C, and significant fluctuations in properties of specimens heat-treated at 145 °C.

Keywords: cellulose; heat treatment; hornification; silver nanosuspension; thermal degradation

1. Introduction

Preliminary studies on heat treatment of wood were carried out more than a century ago with an aim to improve some of the troublemaking drawbacks of wood [1]. However, heat treatment methods of wood only became more elaborated and industrially developed in recent decades [2–6].

Changes that occur during the heat treatment process improve dimensional stability and biological resistance against fungal attack as two main drawbacks of wood [7,8]. However, degradation in the main cell-wall polymers negatively impacts some other properties, such as bending and impact strengths [2]. Therefore, finding optimal treatment conditions, under which maximum improvement in drawbacks are achieved with the lowest negative effects on other properties, is still under progress. When heat treatment takes place at mild thermal conditions, it is reported that semi-crystalline cellulose regions change to crystalline [9]. At the same time, polycondensation reactions and cross-linking were noticed in lignin structure [9,10].

Nanotechnology seems to have remarkable potential in producing a new generation of materials with enhanced properties [11]. Nanomaterials have a high surface–volume ratio that enables them to show greater activities in surface-related phenomena compared to bulky systems with an identical mass [12–16]. The change in material properties is primarily due to the large interfacial area, which is developed per unit of volume, since the level of added particles is reduced to nanometres. Nanomaterials enhance the properties of the original material, show a great compatibility with the traditional materials, and cause a limited alteration of their original features [17–21].

Nanosized metals can basically be synthesized by mainly using two chemical approaches: (i) solution-based synthesis (sol-gel, sonochemical, and solvothermal) and (ii) vapour-based synthesis (combustion and chemical vapour deposition) [22–27]. Their use in wood has the objective to enhance its physico-mechanical properties and its durability against microorganisms, since it is generally acceptable that nanosized metals may interact with the bacterial elements, leading gradually to cell death [19,28] or even to a disruption of the enzyme function [18,28]. A common practice is to disperse the nanosized metals in an organic polymer resin in order to form a nanocomposite. A key factor in this process is the proper dispersion of nanoparticles in order to obtain maximum improvements in wood properties. Nanosized materials, such as metal nanoparticles (gold, copper, and silver) and metal oxides (zinc and aluminium), are nowadays widely applied to provide wood protection and to facilitate wood modification.

As far as copper is concerned, while traditional alkaline copper preservatives are solubilized in aqueous solution, nano-copper compounds are initially dispersed in water, and subsequently, the suspension is used for the treatment of wood. A fixation of nano-copper compounds primarily occurs through the deposition on cell wall layers and in pits [29,30]. It was reported that, in some cases, fungi might not be able to recognize copper nanoparticles. Once nanoparticles enter the fungal cell wall, they form a reactive oxygen species with the fungus cell. In addition, nanoparticles may also undergo dissolution and, thereby, interfere with homeostatic processes within the fungal cell [31,32]. Akhtari and Nicholas exposed wood to a termite attack and found that nano-copper formulation could reduce the mass loss from 46.8 to 0.2% [33]. Treating wood with nano-copper oxide in the presence of polystyrene improved the dimensional stability [34].

The interest in silver nanoparticles for different types of applications has grown worldwide [35]. This type of nanoparticle has also gained popularity in the improvement of wood properties and has been the subject of numerous studies. The possibility to improve the sorption behaviour of wood by applying a nano-silver-based compound was recently studied [36]. The compound reduced the total sorption of water vapour to a great extent. Similar results were also reported elsewhere [37,38]. Silver nanoparticles were applied to improve the durability in a series of tropical series [38]. In all cases, the treated woods were classified as highly resistant for white decay fungi, as opposed to untreated wood, of which the mass losses were more than 20%.

Zinc-based nano-compounds have also been applied to wood to improve its durability [39]. It was found that the mass loss due to fungi and termite attacks was significantly inhibited by the zinc-based preparations. In another study, lime wood treated with a zinc-based nano-compound had about a 56% higher resistance against *Trametes versicolor*—A white-rot fungus—And a 40% higher resistance against *Coniophora puteana*—A brown-rot fungus [40,41].

In other studies, nano-compounds based on zinc and copper have been applied to examine the resistance against mould and termite [39,42]. The results revealed that the compound based on zinc is more effective in terms of termite mortality, the inhibition of termite feeding, and the decay by the white-rot fungus. Nano-compounds based on zinc seem to be most appropriate for wood protection [43,44]. Bak and Nemeth [45] studied the efficacy of five different nanoparticles, namely (zinc oxide, zinc borate, copper borate, silver, and copper) against fungi. They found that the most effective nanoparticle treatments were those containing borate. However, only the zinc oxide, silver, and copper nanoparticles showed a resistance to leaching and, therefore, they concluded that only the zinc oxide provided effective protection after leaching.

In our previous study, the physical and mechanical properties of thermally modified beech wood were investigated, a popular and abundant industrial hardwood species, impregnated with silver nanosuspension, and we examined their relationship with the crystallinity of cellulose [46]. The aim of the present work, therefore, was twofold:

- i. To investigate if any potential increase in thermal conductivity, due to silver nano-particles, can be beneficial in both achieving positive effects of mild thermal conditions, and at the same time, avoiding high degradation in cell-wall polymers at higher temperatures. Therefore, target temperatures were planned as low as 145 °C, 165 °C, and 185 °C to make sure that the potential effects of an improved thermal conductivity in the small dimension specimens would be detectible. Temperatures below 145 °C would hardly affect wood, and temperatures higher than 185 °C would be too high to clearly demonstrate the effects of impregnation of small specimens with silver nanosuspension;
- ii. To compare the results obtained in our previous study, which utilized a hardwood species, with the results of the present study, which utilized a softwood species with inferior properties, namely pine, and to identify potential different behaviour between hardwood and softwood species.

2. Materials and Methods

2.1. Sample Preparation

Five Scots pine planks (*Pinus sylvestris* L.) were purchased; they were originally grown in Republic of Tuva (Russia), located in south-central Siberia, Asia. The plunks were from the sapwood portion of trees. Density of the wood was 0.47 g·cm⁻³. The amount of acetone soluble extractives was 5.2%. The harvesting area was about 50° north latitude and 90° east longitude. They were already seasoned, so they were kept for two months at Shahid Rajaee University campus (20 ± 3 °C; 40 ± 3% relative humidity) to make sure their moisture contents were equal in all parts. Twenty one specimens for each of the tests were cut and randomly categorized into seven treatments; these include control specimens (not treated), heat-treated (HT) specimens, and heat-treated specimens impregnated with nanosilver suspension (NS-HT), both at three temperatures, 145 °C, 165 °C, and 185 °C. All specimens were seasoned for three months at room conditions to about 8% moisture content to eliminate the effects of thermo-hygro-mechanical behaviour on the results [47].

2.2. Nanosilver Impregnation

Specimens were first cut to size for different tests and then, impregnated with a 400-ppm silver nanosuspension. The dimensions of specimens for each test are mentioned in the following sections (Section 2.5). The pH of the nanosuspension was 6–7. Two kinds of surfactants (anionic and cationic) were used as stabiliser of nanosilver clusters. Concentration of surfactants was equal to nanosilver clusters. The size of 70% of silver nano-particles ranged from 20 to 100 nm. Specimens were put in a sealed pressure vessel to be impregnated. First, a 0.07 MPa vacuum pressure was applied for twenty minutes. Then a 0.25 MPa pressure was applied for thirty minutes (Figure 1). Once impregnated, they were kept in room conditions (25 ± 3 °C; 35 ± 3% relative humidity) to be dried for a period of three months. Separate specimens were impregnated simultaneously for checking the depth of penetration of nanosuspension. Immediately after the impregnation, these specimens were cut in half to visually investigate the depth of penetration of nanosilver suspension. It was observed that all throughout the specimens (and all of the inner parts) were fully impregnated with the suspension, confirming that the suspension had reached all of the surface and inner parts of the specimens equally.

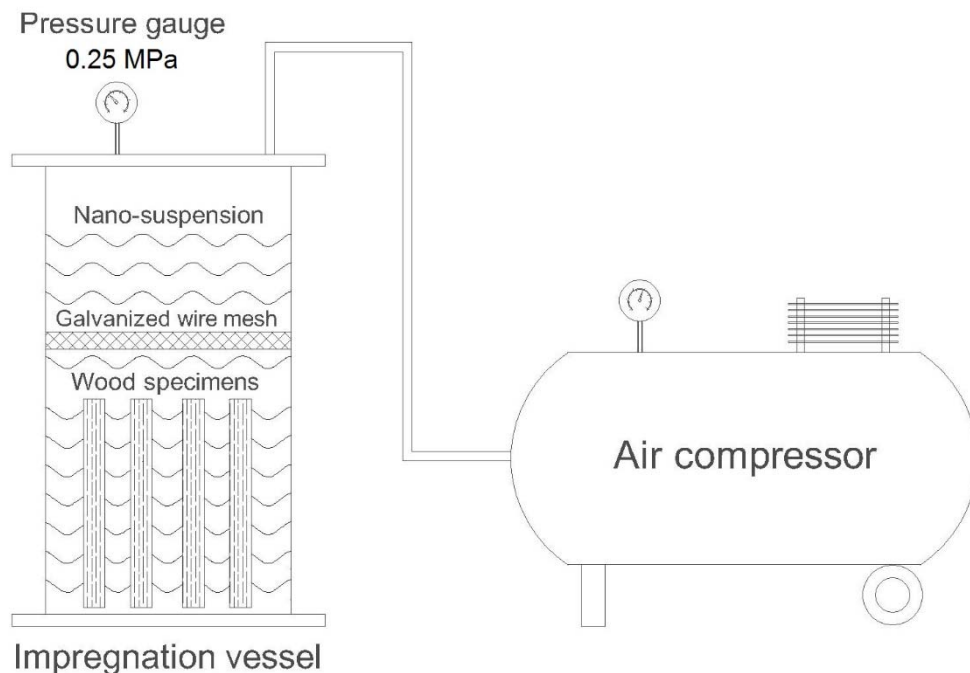


Figure 1. Laboratory scale pressure vessel for impregnating of specimens cut to size for different tests.

2.3. Heat Treatment

Specimens were heat-treated under hot atmospheric air, using a laboratory oven and under atmospheric pressure (model Memmert UFE 700). No water or water spray were used during heat treatment. Target temperatures were planned as low as 145 °C, 165 °C, and 185 °C to make sure that the potential effects of an improved thermal conductivity in the small dimension specimens would be detectable. HT-145 and NS-HT-145 specimens were heated for 24 h at 145 °C. For specimens HT-165 and NS-HT-165, as well as HT-185 and NS-HT-185, another approach was made. Specimens were first heat treated at 145 °C (24 h duration) and afterwards were heat-treated for four hours at 165 °C or 185 °C. A narrow strip of three-layer plywood was put beneath each specimen to avoid direct contact of the specimen with the metal tray of the laboratory oven. Once heat treatment was done, the door of the oven was opened, by an inch, to allow the specimens inside to slowly cool off. Then, all specimens were kept in room conditions (25 ± 3 °C; $35 \pm 3\%$ relative humidity) for four weeks to reach moisture content of 6.5%.

2.4. Total Crystallinity Index (TCrI)

Absorption bands in the Fourier Transform Infrared Spectroscopy (FTIR) have long been used to determine chemical compositions of materials. As for cellulose, different FTIR spectroscopy methods have been developed to characterize small differences in the structures of crystalline cellulose, including dynamic, and static [48], and to establish relation between certain FTIR bands to crystalline and amorphous cellulose [49,50]. In the present study, the total crystallinity index (TCrI or TCI) was considered the baseline to measure and report the amount of crystallinity [50–52]. In this index, the band (at 1372 cm^{-1}) is attributed to C-H deformation, and the band at 2900 cm^{-1} is attributed to C-H and CH_2 stretching. To calculate TCrI in this method, the area under C-H band is divided by the area under the band of C-H and CH_2 stretching. The obtained index represents total crystallinity (Equation (1)). No deconvolution was conducted in the measurement of the area under the curve for either of the bands because the above-mentioned bands were distinct and no particular overlapping was observed. TCrI measurement with this method is usually done for cellulose fibres and yarns, though it has also been used for solid wood [50]. However, apart from other objectives to measure some physical and mechanical properties of heat-treated and nanosilver-impregnated specimens,

the present study used this method to give a primarily experiment on the potentiality of measuring total crystallinity using this method. X-ray diffraction (XRD) was not carried out in this study, but it is reported that a linear relationship exists between the results from TCrI with those obtained from XRD [53]. Still, further studies may be carried out with an aim to compare the results of crystallinity measurement based on the above-mentioned two methods.

$$\text{TCrI} = \frac{\text{area under the curve in band } 1372 \text{ cm}^{-1}}{\text{area under the curve in band } 2900 \text{ cm}^{-1}} \quad (1)$$

2.5. Physical and Mechanical Properties

Specimens were first cut to size, and then impregnated with nanosilver or heat-treated. Specimens were weighed with a digital scale (0.1 g precision), both before and after impregnation with nanosilver and heat treatment processes to calculate silver nanosuspension uptake and mass loss in each treatment. Physical and mechanical tests were carried out based on ASTM D0143-94 standard specifications [54]. For modulus of rupture (MOR) and modulus of elasticity (MOE), specimen size was $25 \times 25 \times 410$ (mm) centre-point loading bar, and for compression strength parallel to the grain, specimen size was $25 \times 25 \times 100$ (mm). Tests were carried out at room conditions (25 ± 3 °C; $35 \pm 3\%$ relative humidity). Loading was applied through the bearing block to the tangential surface nearest the pith. Modulus of rupture (MOR), modulus of elasticity (MOE), and compression strength parallel to the grain ($P_{c||}$) were calculated using Equations (2)–(4), respectively.

$$\text{MOR} = \frac{1.5 FL}{bd^2} \text{ (MPa)} \quad (2)$$

$$\text{MOE} = \frac{FL^3}{4bd^3D} \text{ (MPa)} \quad (3)$$

$$P_{c||} = \frac{F_{\max}}{A} \text{ (MPa)} \quad (4)$$

where F : Maximum force at first failure; L : Span length; b : Width of specimen; d : Thickness of specimen; D : Deflection at failure; F_{\max} : Maximum force; A : Cross-section area of specimen.

Physical properties of water absorption and thickness swelling were measured and calculated with Equations (5) and (6)

$$\text{Water Absorption} = \frac{M_x - M_i}{M_i} \times 100 \text{ (\%)} \quad (5)$$

where M_x and M_i are masses (g) at time x and initial mass (g), respectively.

$$\text{Thickness Swelling} = \frac{T_x - T_i}{T_i} \times 100 \text{ (\%)} \quad (6)$$

where T_x and T_i are thickness of specimens (mm) at time x and the initial thickness (mm), respectively.

2.6. Statistical Analysis

SAS software program was used to carry out statistical analysis in the present study (version 9.2; 2010). To discern significant difference among different treatments and produced panels, one-way analysis of variance was performed at 95% level of confidence. Then, Duncan's multiple range test (DMRT) was done for grouping among treatments for each property. In order to find degrees of similarities among different treatments based on all properties studied here, hierarchical cluster analysis from SPSS/18 (2010) software was used. For graphical statistics (fitted-line, contour, and surface plots), Minitab software was utilized (version 16.2.2; 2010).

3. Results and Discussion

3.1. Physical and Mechanical Properties

By taking into account the mass measurements before and after the impregnation, silver nanosuspension uptake was measured to be $0.28 \pm 0.02 \text{ g/cm}^3$. Based on the grouping of Duncan's Multiple Range test at 95% level of confidence, mass loss increased significantly, as the treatment temperature increased (Figure 2). At the temperatures of 145 °C (3.3%) and 165 °C (7.5%), low and statistically insignificant difference in mass loss was observed between the un-impregnated and NS-impregnated specimens. However, heat treatment at 185 °C illustrated a mass loss difference of 50% between the un-impregnated and NS-impregnated specimens. Previous studies on beech and poplar wood under the same conditions reported a difference of 11% and 42% between the un-impregnated and NS-impregnated specimens heat-treated at 185 °C, respectively [46,55]. Heat treatment of wood can also cause oxidation and burning out the extractives, and evaporation of moisture content as well, eventually increasing mass loss. Therefore, part of the mass losses measured can be attributed to other components of wood (such as different extractives, and moisture content) other than cell-wall polymers (cellulose, hemicelluloses, and lignin), especially at low temperature of 145 °C. However, only comparing degradation in three major cell-wall polymers, the mass losses at temperatures of 145 °C and 165 °C are mostly attributed to degradation of hemi-cellulose and lignin, as cellulose is reported to have higher resistance against thermal degradation [46,55–60]. In this connection, intensities of finger print region in wave number $1750\text{--}1500 \text{ cm}^{-1}$ are mainly related to C = O stretch in ketones, carbonyls, and ester groups, and in aromatic skeletal vibration as well, all related to hemicelluloses components. Figure 3a,b clearly shows significant difference in intensities of these wave range, indicating that hemicellulose was significantly affected at all temperatures, as a results of heat treatment. Moreover, bands of different curves for the six heat-treated specimens demonstrated significant intensities at 1595 cm^{-1} and 1512 cm^{-1} , both related to aromatic rings in lignin (Figure 3a,b) [61,62]. The significant difference in the intensities at these bands was also corroborating evidence of the effect of heat treatment on lignin.

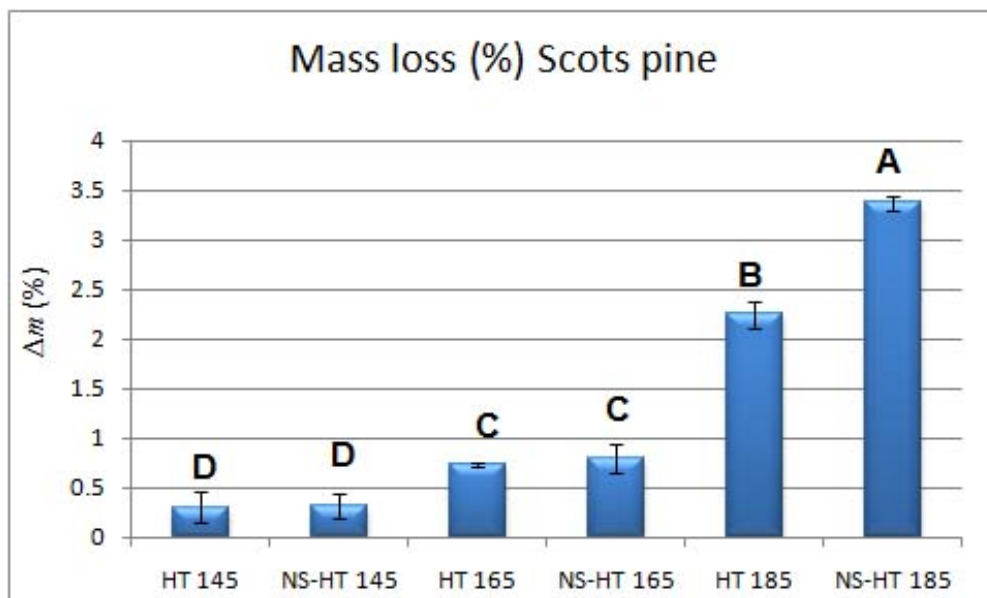


Figure 2. Mass losses (%) in pine specimens heat-treated at 145, 165, and 185 °C and impregnated with silver nanosuspension. (HT = heat-treated at a determined temperature; NS = nano-silver impregnated. Letters on each column represent statistical groupings of mean values based on Duncan's Multiple Range test at 95% level of confidence. Error bars represent standard deviation).

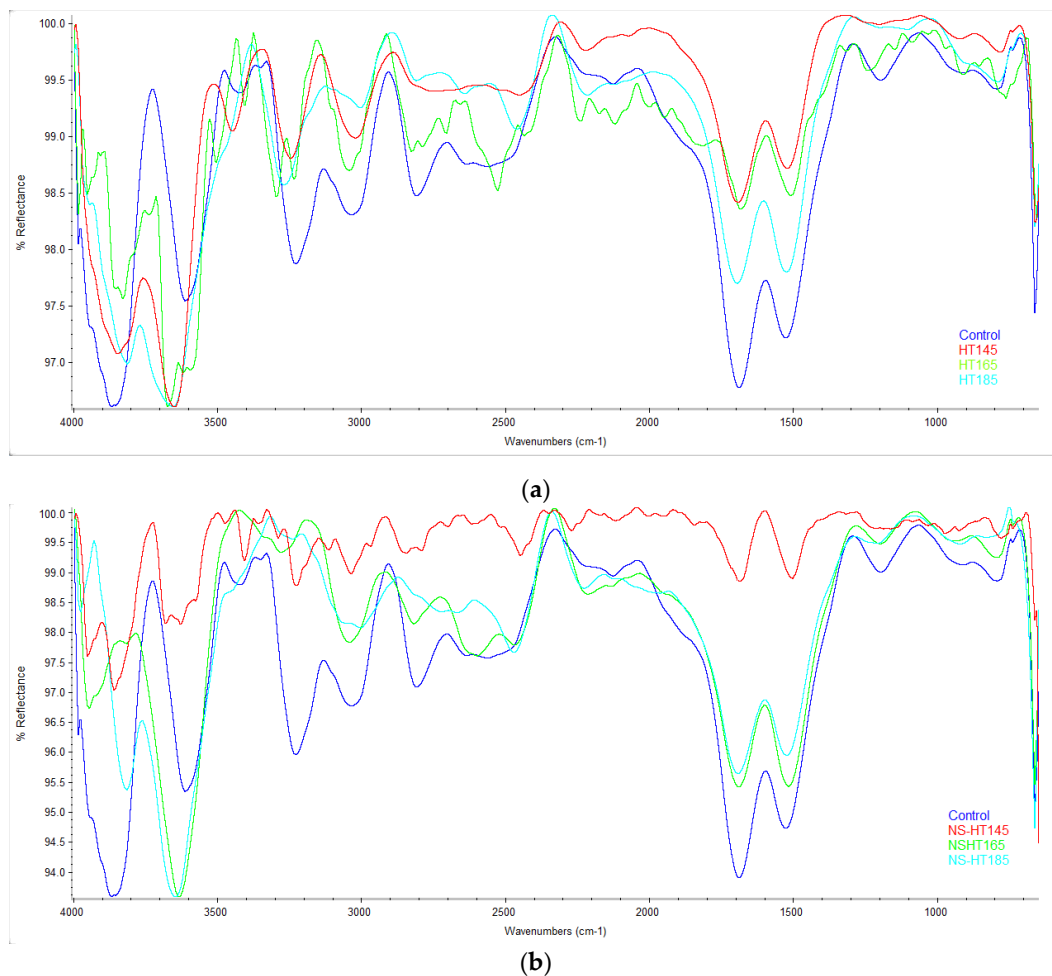


Figure 3. Infrared spectra of control and heat-treated (a) and control and NS-impregnated heat-treated (b) Scots pine specimens (HT = Heat-treated; NS = nano-silver impregnated).

All heat-treated specimens showed significant lower volumetric swelling (VS) in comparison to the control specimens (Figure 4a,b), and a decreasing trend in VS was observed along with the increase in temperature. The decrease in VS was partially attributed to the irreversible hydrogen bonding in the course of water movements within the pore system of cell walls, forming rather permanent bonds with hydroxyl groups of cell-wall components and making them unavailable for water molecules, eventually decreasing hygroscopicity in wood [63]. Intensities of wave numbers of 3300–3100 cm⁻¹ and 1600 cm⁻¹ are related to O-H stretch and hydroxyl groups [61,62]. FTIR spectra of the treatments in the present study demonstrated distinct fluctuations in intensity, indicating that the hydroxyl groups at these bands were unavailable to make bonds with water molecules (Figure 3a,b). This was considered one of the main reasons of the significant decrease in VS in all heat-treated specimens. VS values followed no distinct pattern between the un-impregnated versus NS-impregnated specimens. VS values in pine specimens generally showed lower values in comparison to beech specimens studied previously [46,55]. This was attributed to lower woody mass in pine wood in comparison to beech wood. This was also associated with higher water absorption (WA) values in pine specimens in comparison to beech, indicating the impact of lower density and higher cell cavities on both physical properties of VS and WA. As to water absorption values, all heat-treated specimens illustrated higher WA values after 24 h of immersion in water in comparison to the control specimens, though no regular pattern was observed (Figure 4c,d). This may be attributed to occurrence of micro-checks and cracks that were reported as a result of heat treatment in hardwood species [64,65]. However, microscopic imaging should be done to come to a final firm conclusion with regard to WA.

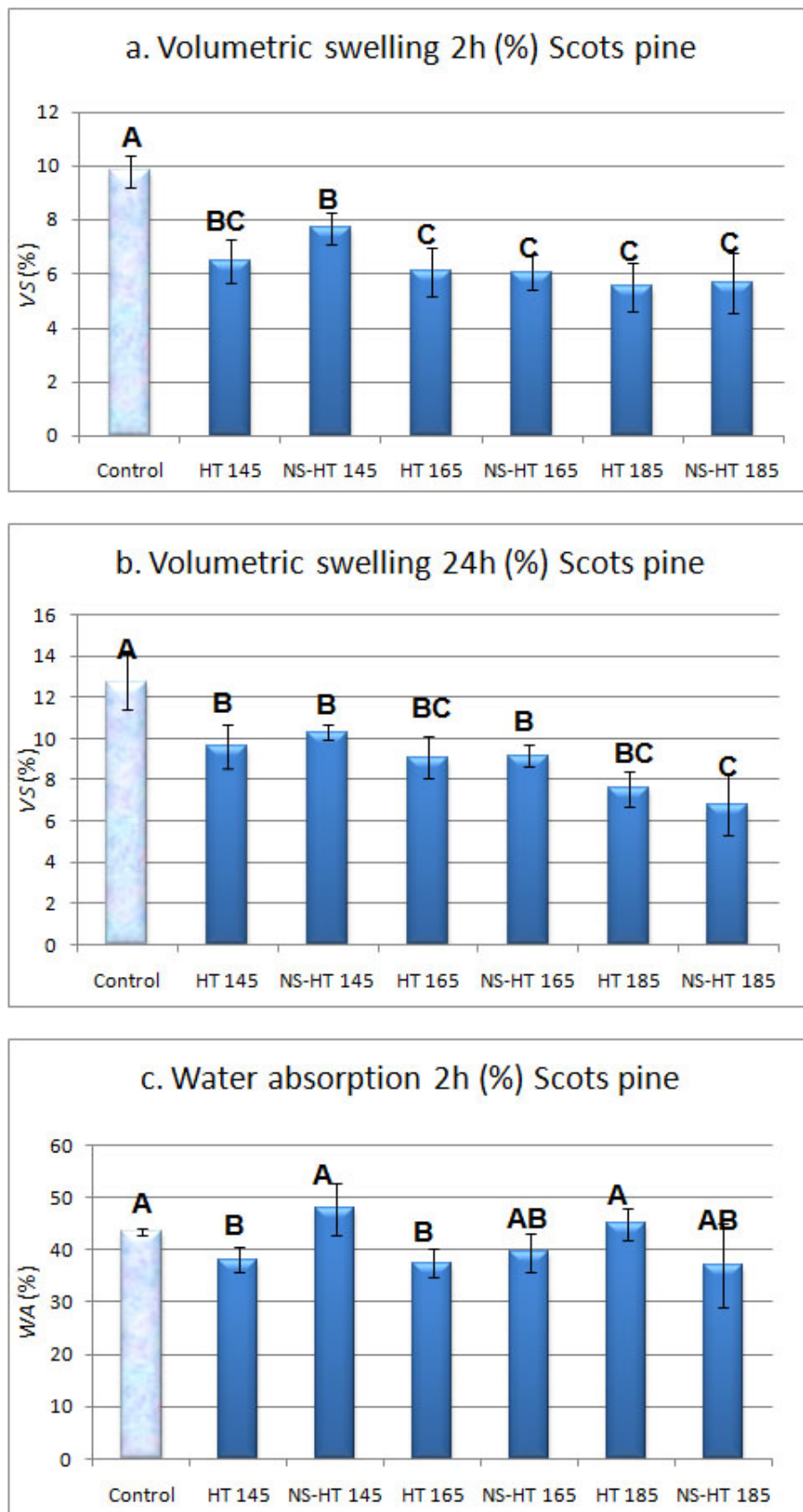


Figure 4. Cont.

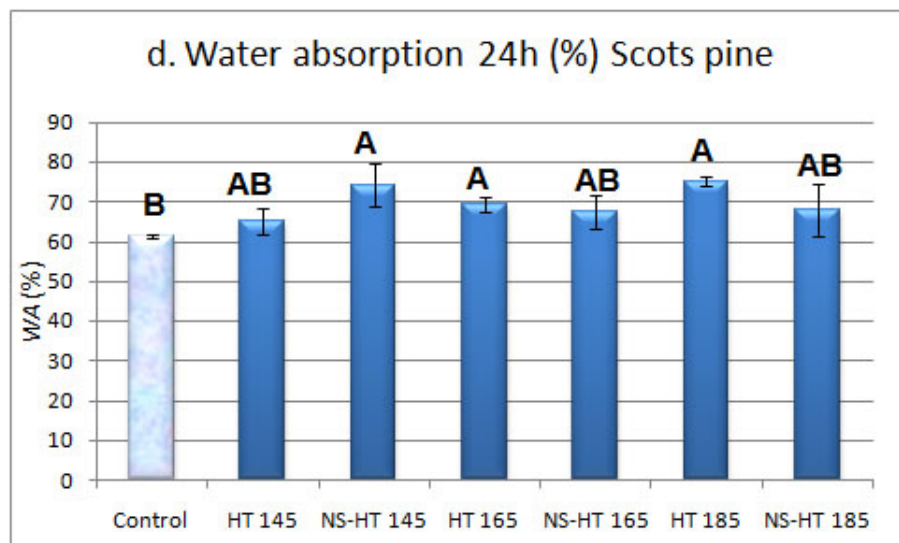


Figure 4. Physical properties of volumetric swelling after 2 h (a) and 24 h (b), as well as water absorption after 2 h (c) and 24 h (d), in Scots pine specimens heat-treated at 145, 165, and 185 °C and impregnated with silver nanosuspension. (HT = heat-treated at a determined temperature; NS = nano-silver impregnated. Letters on each column represent statistical groupings of mean values based on Duncan's Multiple Range test at 95% level of confidence. Error bars represent standard deviation).

All four mechanical properties studied here decreased after heat treatment at 165 °C and 185 °C, though the decreasing values were not statistically significant in some cases (Figure 5a–d). This was attributed to degradation of cell-wall polymers [2]. However, heat treatment at 145 °C did not have a regular effect on mechanical properties; some properties even increased, such as MOR and impact bending, though crystallinity decreased (Figure 6). This was opposite to the increased crystallinity at 145 °C that was observed in beech specimens [47,55]. The increase in some of the properties can partly be attributed to hornification [63]. This phenomenon is the consequence of irreversible hydrogen bonding during which, the mobility of molecular chains within wood cell wall is increased, resulting in structural rearrangement [56,57]. During the rearrangement, and along with removal of water molecules because of the heat treatment, irreversible hydrogen bonds are formed between adjacent carbohydrate elements [63,65–68]. In the present study, the improving effects caused by hornification mitigated the negative effects of thermal degradation of cell-wall polymers, eventually keeping the values at the same range or even more than control specimens. Another phenomenon that may have influenced the process is the glass transition of lignin [2,69,70]. Amorphous polymers change their glassy state to a gel-like state at a point where the whole structure gradually softens; this point is called the glass transition temperature. In this transition process, the covalent bonds between hemi-cellulose and lignin are broken, and lignin fragments are formed with low molecular weight and high reactivity [9,11]. Though in some literature it is reported that glass transition of lignin occurs with increasing temperature up to 200 °C based on the moisture content of wood specimens [71–73], some others indicated glass transition (broad transition, α_1) temperatures of 80 °C and 100 °C for spruce and sugar maple, respectively [70]. In this regard, intensities of all six heat-treated specimens at bands 1595 cm^{-1} and 1512 cm^{-1} , which are both related to aromatic rings of lignin, illustrated significant difference with that of control specimen (Figure 3a,b). One of the effects of this significant difference in the aromatic ring can be translated into the changes that occurred during glass transition of lignin. Therefore, it can be hypothesized that the improvement in some of the properties can also be partially attributed to repolymerisation of lignin during which these fragments were bonded together, eventually improving the overall strength of wood structure.

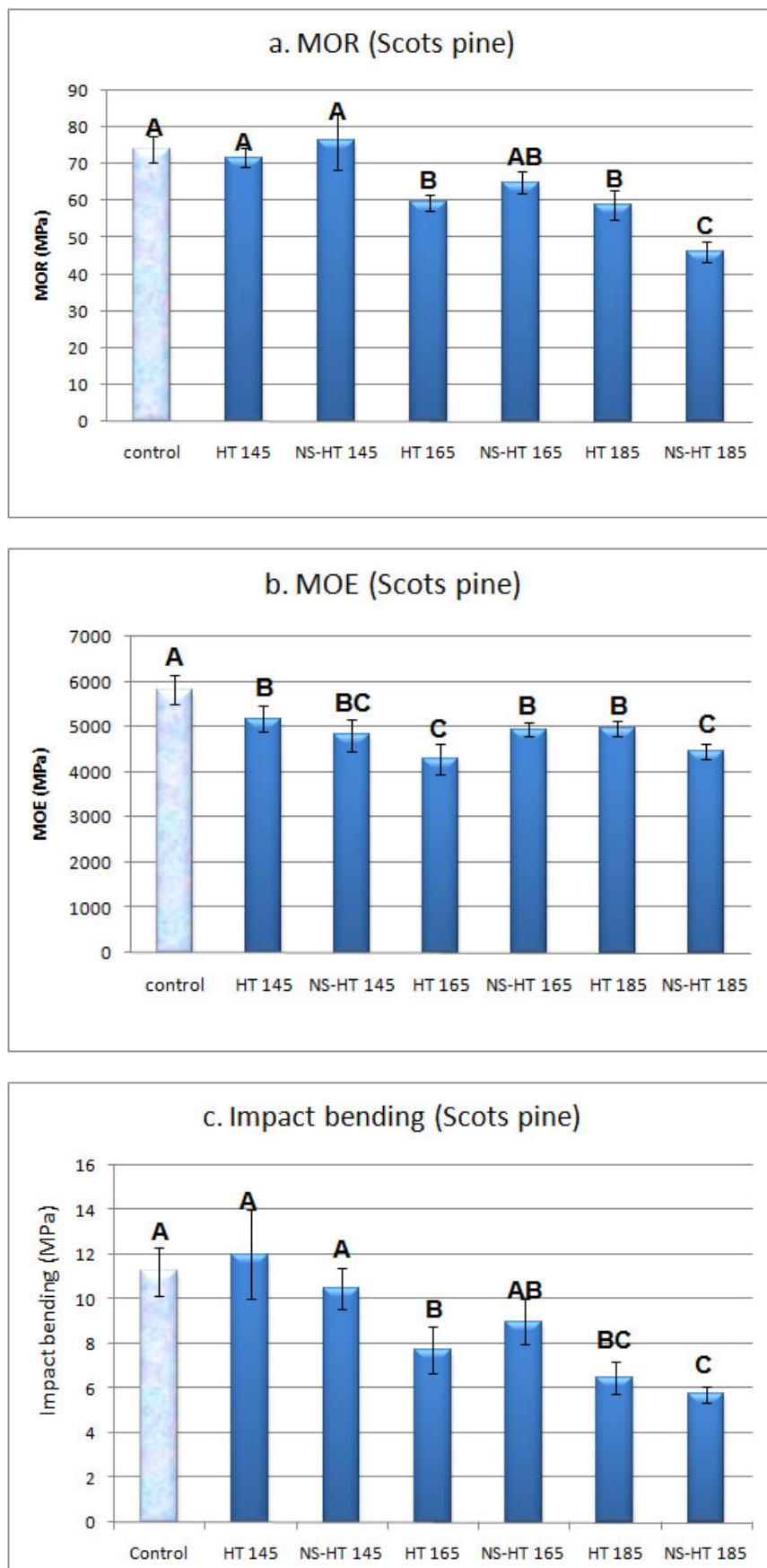


Figure 5. Cont.

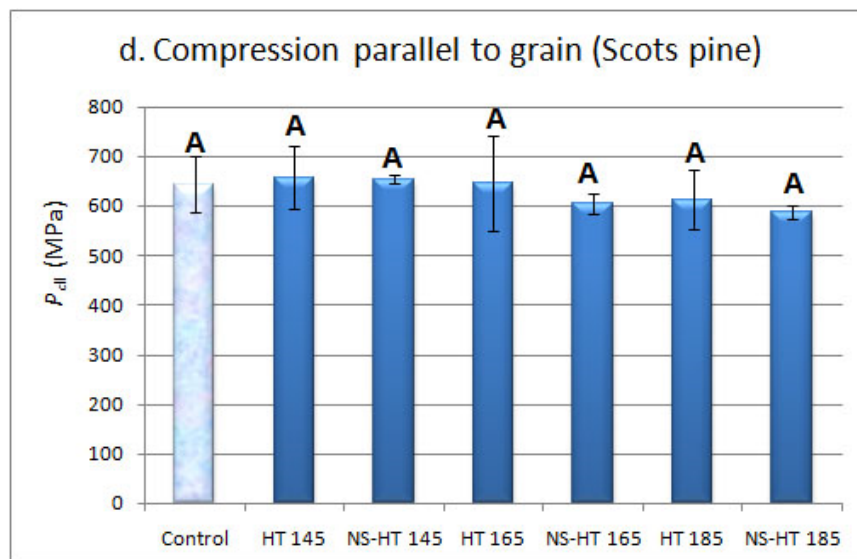


Figure 5. Mechanical properties, including modulus of rupture (a), modulus of elasticity (b), impact bending (c), and compression strength parallel to grain (d) in pine specimens heat-treated at 145, 165, and 185 °C and impregnated with silver nanosuspension (HT = heat-treated at a determined temperature; NS = nano-silver impregnated). MOR = modulus of rupture; MOE = modulus of elasticity. Letters on each column represent statistical groupings of mean values based on Duncan's Multiple Range test at 95% level of confidence. Error bars represent standard deviation).

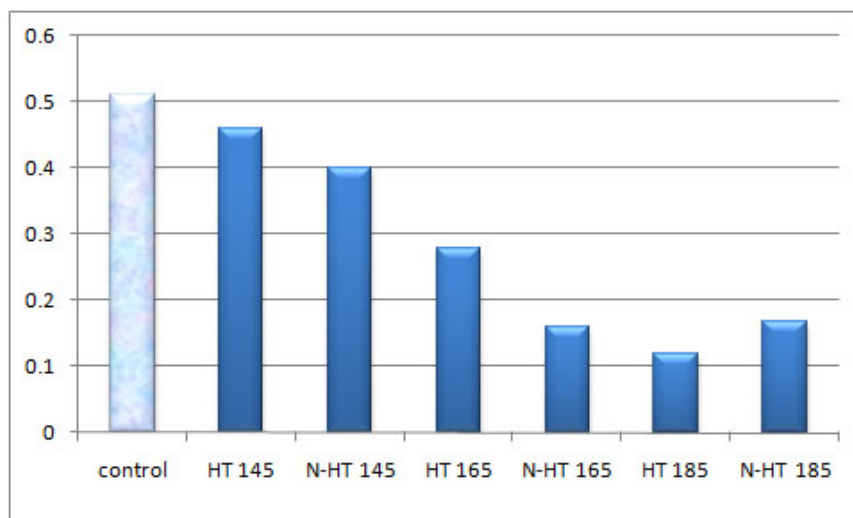


Figure 6. Crystallinity in control along with six heat-treated pine specimens (HT = heat-treated at a determined temperature; N = nano-silver impregnated).

Increase in thermal conductivity both in solid wood and engineering panels due to addition of metal and mineral nano-particles was previously reported and therefore, thermal conductivity was not directly measured in this study. However, its significant effect on MOR and mass loss values in specimens heat-treated at 185 °C was observed. The effects of heat treatment on other properties and at the other two temperatures did not follow a regular trend; that is, both increasing and decreasing trends were observed. These fluctuations are originated on the interacting effects of different phenomena that simultaneously affect the properties, like degradation of cell-wall polymers, hornification, as well as a decrease in the number of hydroxyl groups.

3.2. FTIR Analysis

Infrared spectra were in close agreement with the above-discussed fluctuations in both mechanical and physical properties (Figure 3a,b). Clear and distinctive differences were observed in wave numbers 3350–3000 cm^{-1} , and these were related to hydroxyl groups of cell-wall polymers. Important differences were also observed in the intensities of finger print region of wave number 1700–1500 cm^{-1} (C = O stretching); this is the case in both un-impregnated and NS-impregnated treatments. It is worth to mention that the peak of 1733 cm^{-1} was reduced in intensity in all heat-treated wood samples. This particular wave number is assigned to the stretching vibrations of carbonyl groups; these belong mainly to hemicellulose. HT145 and HT165 treatments revealed more similarity at this wave number in comparison to HT185, showing that degradation at these two temperatures mostly happened in hemicellulose and lignin. However, impregnation with silver nanosuspension in NS-HT165 made more cellulose to be degraded and therefore, in the NS-impregnated graph (Figure 3b), NS-HT165 showed more similarity to NS-HT185. It should be taken into account that crystallinity measurement in the present study demonstrated a decrease in the absolute values of crystalline cellulose, as the heat treatment temperature increased (Figure 6). In this connection, another study that used TCRI reported that crystallinity decreased in hot-pressed poplar as a result of heat treatment at 150 °C and 200 °C temperatures [50], which are near the temperature range in the present study (namely, 145 °C and 185 °C). However, a previous study indicated that the relative amount of crystalline cellulose increases due to heat treatment [9]. The cited authors further argued that it is still a matter in dispute whether the increase is attributed to the degradation of more amorphous cellulose than that of crystalline cellulose, or it is due to crystallization of part of amorphous cellulose, adding to the absolute amount of crystalline cellulose. It is also possible that both phenomena occur at the same time. With due consideration of the findings on the effects of heat treatment on crystallinity in the present and previous studies, it can be concluded that there is still scepticism on the extent of the effects of heat treatment at mild temperatures on cellulose crystallinity. Based on the above mentioned facts, further studies should be carried out to specifically compare relative and absolute values of crystallinity using two methods, namely TCRI measurement (the method described in present study), and X-ray differentiation (XRD). In these supplementary studies, heat treatment of different hardwood and softwood species at a wider temperature range may be carried out for comparison purposes, including mild temperatures (below 200 °C), and higher temperatures as well. Comparison of the results, thereof, is essential to come to a conclusion on the increasing or decreasing trend in crystallinity of cellulose, and authenticity of TCRI based on intensities of FTIR spectra as well. Moreover, further studies on absolute amounts (not relative amounts) of crystalline and amorphous cellulose at different heat-treatment temperatures should also be carried out to conclude on this issue.

3.3. Potential Effects of Species

Comparison between the results of the present study with those previously carried out under the same temperatures and conditions on beech wood (as a popular industrial hardwood species) demonstrated lower weight losses as a result of heat treatment in all treatments [46]. At temperatures of 145 °C and 165 °C, neither of the species (beech or Scots pine) showed difference in weight loss between un-impregnated and NS-impregnated specimens. However, at a temperature of 185 °C, the difference was higher in pine wood in comparison to beech wood. Though fluctuations can be observed between the two species, the overall decreasing trend in VS was obvious in both species. All mechanical properties of beech were significantly higher than their counterparts in pine wood, which is only natural considering the higher density of beech wood (0.62 $\text{g}\cdot\text{cm}^{-3}$ and 0.47 $\text{g}\cdot\text{cm}^{-3}$ for beech and Scots pine wood, respectively).

FTIR spectra of both species demonstrated high and significant alteration in the intensities of wave numbers 1750–1500 cm^{-1} . Wave number 1738 cm^{-1} is related to C = O stretching in carbonyl and ester groups of hemicellulose [61,62]. Considering the fact that hemicellulose of hardwood contain mostly xylans, while that of softwood species contain glucomannans, the significant difference in

intensities of the control spectra of these two species would be explained. Heat treatment at different temperatures seemed to affect differently on these two species, which can partially be related to the difference in these building blocks mentioned above. However, further studies consisting atomic absorption analysis should be carried out to quantitatively analyse alteration in each element, in order to conclude how, and to what extent, each ingredient can be affected and degraded.

Similar clear differences were observed between the intensities at wavelengths of 1600 and 1500 cm^{-1} , which are both related to aromatic compounds that are plenty in lignin structure. The difference in the above-mentioned intensities is mainly attributed to the difference in guaiacyl and syringyl units that form lignin in softwood and hardwood species. However, further supplementary studies, specifically focused on chemical composition of lignin and their alterations as a result of thermal degradation at different temperatures, should be carried out to be in a position to conclude on the fluctuations in intensities of FTIR spectra.

Heat treatment at different temperatures resulted in significantly different effects on intensities discussed above. In this connection, it is to be noted that, in both the present study, and the previous study on beech wood as well [46], heat treatment was carried out at mild temperatures (below 200 °C). This means that the thermal degradation in cell-wall polymers mainly occurred in hemicellulose and lignin compounds, as thermal degradation occurs in cellulose at higher temperatures [9,46,55,60]. The differences in building blocks of hemicellulose and lignin in softwood and hardwood species that were discussed above can clarify the great differences on the effects of heat treatment at each temperature on fluctuations in wave number intensities.

3.4. Analytical Statistics of Treatments

Fitted-line plot between crystallinity values and mechanical properties revealed that R-square values were not very high. The highest correlation was found between crystallinity and impact bending (77.7%) (Figure 7). Fitted-line plot between crystallinity and VS was 71% (Figure 8). This can partially be attributed to the formation of irreversible new hydrogen bonds. The rather low R-square indicated that there were also other factors (along with crystallinity) that affected the mechanical properties; the interactions between these factors did not let R-square to go higher than about 77%. Contour and surface plots also presented direct three-sided relationships among mechanical properties (Figure S1) and physical properties (Figure S2) versus ATR-crystallinity (Attenuated Total Reflectance). Although, some minor distortions were observed, which were related to the interaction of different contradicting impacts of heat treatment, such as degradation of cell-wall polymers on one side and formation of irreversible new hydrogen bonds between hemi-cellulose and lignin on the other.

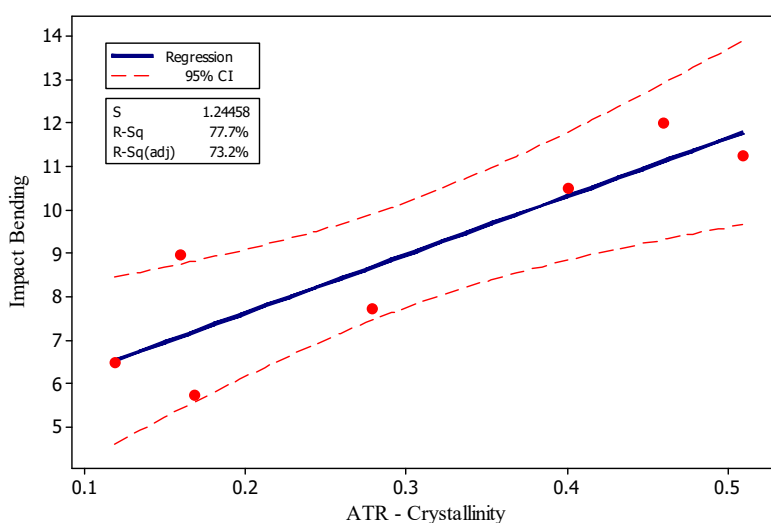


Figure 7. Fitted-line plot between Attenuated Total Reflectance-crystallinity versus impact bending in the seven treatments of Scots pine studied.

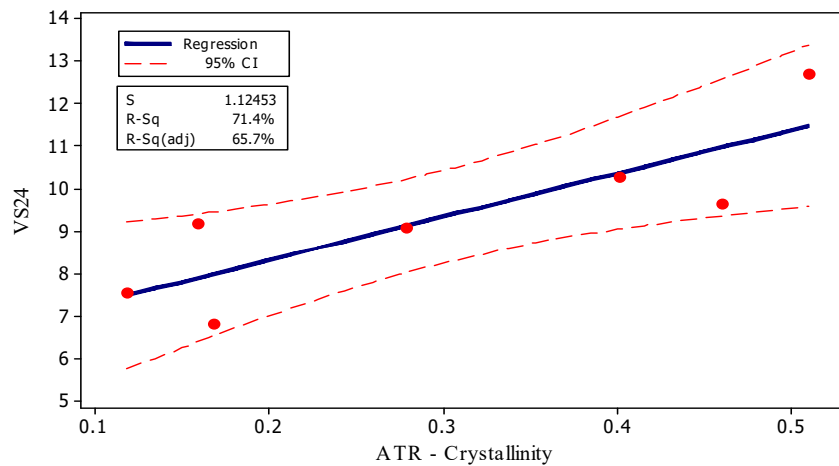


Figure 8. Fitted-line plot between Attenuated Total Reflectance-crystallinity versus physical properties of VS in the seven treatments of Scots pine studied (VS = volumetric swelling after 24 h-immersion in water).

Cluster analysis related to the four physical and four mechanical properties, and the ATR-crystallinity values illustrated that HT145 and NS-HT145 treatments were clustered very close to control specimens (Figure 9). This indicated that although mass loss measurement showed slight thermal degradation at 145 °C, other effects of heat treatment on cell-wall polymers, such as hornification and formation of new hydrogen bonds, managed to compensate for the loss and, therefore, the overall properties could be considered rather the same as the control specimens. Similar clustering of HT145 treatments was reported for beech wood [46]. Therefore, it can be concluded that heat treatment at this temperature can only slightly affect the overall properties in low and medium density wood species. Moreover, the change on the properties is not necessarily negative while heat treatment can form new irreversible bonds between cell-wall polymers, eventually improving a number of properties at 145 °C. However, further studies should be carried out for every species in order to reaffirm this conclusion. Heat treatment at 165 °C and 185 °C illustrated distinctly different clustering compared to the control specimens, revealing significant effect of heat treatment at these two temperatures. Both un-impregnated and NS-impregnated treatments at 165 °C revealed very close clustering, implying that the improved thermal conductivity caused by silver nanoparticles had insignificant effect at this temperature on wood properties. However, the improved conductivity had higher effect at temperatures of 145 °C and 185 °C.

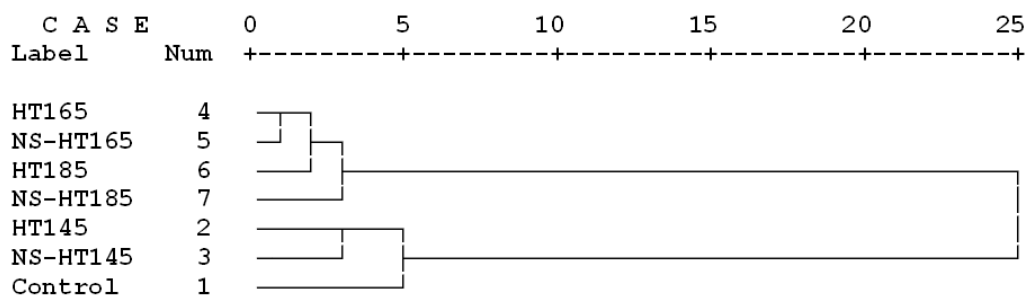


Figure 9. Cluster analysis based on four physical and four mechanical properties, as well as crystallinity values of the seven treatments studied in the present project (HT = heat-treated at a determined temperature; NS = nano-silver impregnated).

4. Conclusions

Cut-to-size Scots pine specimens were impregnated with a 400-ppm silver nanosuspension and were heat-treated at three relatively mild temperatures: 145 °C, 165 °C, and 185 °C. Different physical

and mechanical properties were measured in the six treatments (untreated and NS-impregnated) to be compared with those of control specimens. Results indicated interacting effects of heat treatment on different aspects, the results of which demonstrated opposite outcome at different temperatures. At treatment temperature of 145 °C, low mass loss implied low thermal degradation in lignin and hemicellulose. The low degradation along with hornification, and formation of new bonds between lignin fragments and hemi-cellulose, eventually resulted in an improvement in some of the properties. At temperature of 185 °C, however, high degradation of the main cell-wall components (cellular polymers) overcame the improving effects of hornification; consequently, heat treatment had negative effects on all physical and mechanical properties. FTIR spectra demonstrated significantly different intensities at bands related to hemicelluloses and lignin, providing corroborating evidence on the effects of heat treatment on these cell-wall polymers. The interaction of the above-mentioned thermal effects made it hard to predict the final outcome on the different properties of specimens heat-treated at 165 °C. Based on the results, it was concluded that heat treatment at low temperatures between 145 °C up to about 165 °C can cause hornification, which in turn compensates the negative effects of thermal degradation, to some extent. However, at a temperature of 185 °C, thermal degradation is rather high and cannot be compensated. Impregnation with silver nanosuspension intensifies the above-mentioned effects.

Supplementary Materials: The following are available online at <http://www.mdpi.com/1999-4907/11/4/466/s1>, Figure S1. Contour and surface plots among mechanical properties (impact bending and compression parallel to grain) versus ATR-crystallinity., Figure S2. Contour and surface plots among physical properties (VS after 2 and 24 h immersion in distilled water) versus ATR-crystallinity (VS = volumetric swelling).

Author Contributions: Methodology, H.R.T., S.B.; Validation, H.R.T., H.M., and A.N.P.; Investigation, H.R.T., and S.B.; Writing—Original Draft Preparation, H.R.T., H.M. and A.N.P.; Writing—Review and Editing, H.R.T., and A.N.P.; Visualization, H.R.T., and S.B.; Supervision, H.R.T. and A.N.P. All authors have read and agreed to the published version of the manuscript.

Funding: This research received no external funding.

Acknowledgments: The first author is grateful to the esteemed Familie Kossatz (Hamburg, Germany) for their moral support and inspiration, as well as Alexander von Humboldt Stiftung.

Conflicts of Interest: The authors declare no conflict of interest.

References

1. Tiemann, H.D. The Effect of Different Methods of Drying on the strength of Wood. *Lumber World Rev.* **1915**, *28*, 19–20.
2. Hill, C.A.S. *Wood Modification—Chemical, Thermal and Other Processes*; John Wiley and Sons Ltd.: West Sussex, UK, 2006.
3. Hein, P.R.G.; Silva, J.R.M.; Brancheriau, L. Correlations among microfibril angle, density, modulus of elasticity, modulus of rupture and shrinkage in 16-year-old *Eucalyptus urophylla* × *E. grandis*. *Maderas Cienc. Tecnol.* **2013**, *15*, 171–182.
4. Papadopoulos, A.N.; Taghiyari, H.R. Innovative wood surface treatments based on nanotechnology. *Coatings* **2019**, *9*, 866. [[CrossRef](#)]
5. Papadopoulos, A.N.; Bikiaris, D.N.; Mitropoulos, A.C.; Kyzas, G.Z. Nanomaterials and chemical modification technologies for enhanced wood properties: A review. *Nanomaterials* **2019**, *9*, 607. [[CrossRef](#)]
6. Papadopoulos, A.N. Chemical modification of solid wood and wood raw materials for composites production with linear chain carboxylic acid anhydrides: A brief Review. *BioResources* **2010**, *5*, 499–506.
7. Tjeerdsma, B.F.; Stevens, M.; Militz, H. *Durability Aspects of (Hydro) Thermal Treated Wood*; Document no. IRG/WP 00-4; International Research Group on Wood Preservation: Biarritz, France, 2000.
8. Boonstra, M.J.; Tjeerdsma, B. Chemical analysis of heat treated softwoods. *Holz Roh Werkst.* **2006**, *64*, 204–211. [[CrossRef](#)]
9. Boonstra, M.J.; van Acker, J.; Tjeerdsma, B.F.; Kegel, E.V. Strength properties of thermally modified softwoods and its relation to polymeric structural wood constituents. *Ann. For. Sci.* **2007**, *64*, 679–690. [[CrossRef](#)]

10. Schmidt, O. *Wood and Tree Fungi: Biology, Damage, Protection, and Use*; Springer: Berlin/Heidelberg, Germany, 2006.
11. Roco, M. Nanotechnology's Future. *Sci. Am.* **2006**, *295*, 39–51. [[CrossRef](#)]
12. De Filipo, G.; Nicoletta, F.P.; Chidichimo, G. Flexible nano-photoelectrochromic film. *Chem. Mater.* **2006**, *18*, 4662–4666. [[CrossRef](#)]
13. Taghiyari, H.R.; Soltani, A.; Esmailpour, A.; Hassani, V.; Gholipour, H.; Papadopoulos, A.N. Improving Thermal Conductivity Coefficient in Oriented Strand Lumber (OSL) Using Sepiolite. *Nanomaterials* **2020**, *10*, 599. [[CrossRef](#)]
14. Hassani, V.; Papadopoulos, A.N.; Schmidt, O.; Maleki, S.; Papadopoulos, A.N. Mechanical and Physical Properties of Oriented Strand Lumber (OSL): The Effect of Fortification Level of Nanowollastonite on UF Resin. *Polymers* **2019**, *11*, 1884. [[CrossRef](#)] [[PubMed](#)]
15. Taghiyari, H.; Esmailpour, A.; Papadopoulos, A. Paint Pull-Off Strength and Permeability in Nanosilver-Impregnated and Heat-Treated Beech Wood. *Coatings* **2019**, *9*, 723. [[CrossRef](#)]
16. Mishra, P.K.; Ekielski, A. The self-assembly of lignin and its application in nanoparticle synthesis: A short review. *Nanomaterials* **2019**, *9*, 243. [[CrossRef](#)] [[PubMed](#)]
17. Taghiyari, H.R.; Schimdt, O. Nanotachnology in wood based composite panels. *Int. J. Bioinorg. Hybrid Nanomater.* **2014**, *3*, 65–73.
18. Goffredo, G.B.; Accoroni, S.; Totti, T.; Romagnoli, T.; Valentini, L.; Munafò, P. Titanium dioxide based nanotreatments to inhibit microalgal fouling on building stone surfaces. *Build. Environ.* **2017**, *112*, 209–222. [[CrossRef](#)]
19. Esmailpour, A.; Majidi, R.; Papadopoulos, A.N.; Ganjkhani, M.; Armaki, S.M.; Papadopoulos, A.N. Improving Fire Retardancy of Beech Wood by Graphene. *Polymers* **2020**, *12*, 303. [[CrossRef](#)]
20. Yang, W.; Jiao, L.; Liu, W.; Dai, H. Manufacture of highly transparent and hazy cellulose nanofibril films via coating TEMPO-oxidized wood fibers. *Nanomaterials* **2019**, *9*, 107. [[CrossRef](#)]
21. Taghiyari, H.R.; Majidi, R.; Esmailpour, A.; Samadi, Y.S.; Jahangiri, A.; Papadopoulos, A.N. Engineering Composites Made from Wood and Chicken Feather Bonded with UF Resin Fortified with Wollastonite: A Novel Approach. *Polymers* **2020**, *12*, 857. [[CrossRef](#)]
22. Hill, C.A.S.; Papadopoulos, A.N. A review of methods used to determine the size of the cell wall microvoids of wood. *J. Inst. Wood Sci.* **2001**, *15*, 337–345.
23. Teng, T.; Arip, M.; Sudesh, K.; Lee, H. Conventional technology and nanotechnology in wood preservation: A review. *BioResources* **2018**, *13*, 9220–9252. [[CrossRef](#)]
24. Polleti Papi, M.A.; Caetano, F.R.; Berganini, M.F.; Marcolino-Junior, L.H. Facile synthesis of a silver nanoparticles/polypyrrole nanocomposite for non-enzymatic glucose determination. *Mater. Sci. Eng. C* **2017**, *75*, 88–94.
25. Gupta, A.; Srivastana, R. Zinc oxide nanoleaves: A scalable disperser assisted sonochemical approach for synthesis and an antibacterial application. *Ultrason. Sonochem.* **2018**, *41*, 47–58. [[CrossRef](#)] [[PubMed](#)]
26. Moya, R.; Zuniga, A.; Berrocal, A.; Vega, J. Effect of silver nanoparticles synthesized with NPs Ag-ethylene glycol on brown decay and white decay fungi of nine tropical woods. *J. Nanosci. Nanotechnol.* **2017**, *17*, 1–8. [[CrossRef](#)]
27. Papadopoulos, A.N.; Militz, H.; Pfeffer, A. The biological behaviours of pine wood modified with linear chain carboxylic acid anhydrides against soft rot decay. *Int. Biodegrad. Biodeterior.* **2010**, *64*, 409–412. [[CrossRef](#)]
28. Civardi, C.; Schwarze, F.; Wick, P. Micronized copper wood protection: An efficiency and potential health and risk assessment for copper based nanoparticles. *Environ. Pollut.* **2015**, *200*, 20–32. [[CrossRef](#)]
29. Matsunaga, H.; Kiguchi, M.; Evans, P. Microdistribution of copper carbonate and iron oxide nanoparticles in treated wood. *J. Nanoparticle Res.* **2009**, *11*, 1087–1098. [[CrossRef](#)]
30. Xue, W.; Kennepohl, P.; Ruddick, W. Chemistry of Copper Preservative Treated Wood. In 45th International Group on Wood Protection, St. George, Utah, USA; IRG/WP 14-30651. 2014, pp. 1–8. Available online: <https://www.irg-wp.com/> (accessed on 17 April 2020).
31. Civardi, C.; Kaiser, J.; Hirsch, C.; Muchino, C.; Wichser, A.; Wick, P.; Schwarze, F. Release of copper amended particles from micronized copper pressure treated wood during mechanical abrasion. *J. Nanotechnol.* **2016**, *14*, 1–10. [[CrossRef](#)]
32. Akhtari, M.; Ganjipour, M. Effect of nano-silver and nano-copper and nano zinc oxide on Paulownia wood exposed to white rot fungus. *Agric. Sci. Dev.* **2013**, *2*, 116–119.

33. Akhtari, M.; Nicholas, D. Evaluation of particulate zinc and copper as wood preservatives for termite control. *Eur. J. Wood Wood Prod.* **2013**, *71*, 395–396. [[CrossRef](#)]
34. Jafari, A.; Omidvar, A.; Rasouli, D. The effect of nano copper oxide on physical properties and leaching resistance of wood polystyrene polymer. *J. Wood For. Sci. Technol.* **2018**, *25*, 9–25.
35. He, M.; Chen, M.; Dou, Y.; Ding, J.; Hangbo, Y.; Guoqiang, Y.; Chen, X.; Cui, Y. Electrospun silver nanoparticles-embedded feather keratin/poly(vinyl alcohol)/poly(ethylene oxide) antibacterial composite nanofibers. *Polymers* **2020**, *12*, 305. [[CrossRef](#)] [[PubMed](#)]
36. Mantanis, G.; Papadopoulos, A.N. The sorption of water vapour of wood treated with a nanotechnology compound. *Wood Sci. Technol.* **2010**, *44*, 515–522. [[CrossRef](#)]
37. Mantanis, G.; Papadopoulos, A.N. Reducing the thickness swelling of wood based panels by applying a nanotechnology compound. *Eur. J. Wood Wood Prod.* **2010**, *68*, 237–239. [[CrossRef](#)]
38. Moya, R.; Berrocal, A.; Zuniga, A.; Baudrit, J.; Noguera, S.C. Effect of silver nanoparticles on white rot wood decay and some physical properties of three tropical wood species. *Wood Fiber Sci.* **2014**, *16*, 1–12.
39. Mantanis, G.I.; Terzi, E.; Kartal, S.N.; Papadopoulos, A.N. Evaluation of mold, decay and termite resistance of pine wood treated with zinc and copper based nanocompounds. *Int. Biodeterior. Biodegrad.* **2014**, *90*, 140–144. [[CrossRef](#)]
40. Reinprecht, L.; Vidholdova, Z.; Kozienska, M. Decay inhibition of lime wood with zinc oxide nanoparticles used in combination with acrylic resin. *Acta Fac. Xylogologiae Zvolen* **2015**, *57*, 43–52.
41. Reinprecht, L.; Vidholdova, Z. Biological resistance and application properties of particleboards containing nano-zinc oxide. *Adv. Mater. Sci. Eng.* **2018**, *2018*, 2680121. [[CrossRef](#)]
42. Kartal, S.N.; Green, F.; Clausen, C.A. Do the unique properties of nanometals affect leachability or efficacy against fungi and termites? *Int. Biodeterior. Biodegrad.* **2009**, *63*, 490–495. [[CrossRef](#)]
43. Huang, H.H.; Lin, C.; Hsu, K. Comparison of resistance improvement to fungal growth on green and conventional building materials by nano-metal impregnation. *Build. Environ.* **2015**, *93*, 119–127. [[CrossRef](#)]
44. Terzi, E.; Kartal, S.; Yilgor, N.; Rauptari, L.; Yoshimura, T. Role of various nano-particles in preservation of fungal decay, mold growth and termite attack in wood and their effect on weathering properties and water repellency. *Int. Biodeterior. Biodegrad.* **2016**, *107*, 77–87. [[CrossRef](#)]
45. Bak, M.; Nemeth, R. Effect of different nanoparticle treatments on the decay resistance of wood. *BioResources* **2018**, *13*, 7886–7899. [[CrossRef](#)]
46. Bayani, S.; Taghiyari, H.R.; Papadopoulos, A.N. Physical and mechanical properties of thermally-modified beech wood impregnated with silver nano-suspension and their relationship with the crystallinity of cellulose. *Polymers* **2019**, *11*, 1538. [[CrossRef](#)] [[PubMed](#)]
47. Figueroa, M.; Bustos, C.; Dechent, P.; Reyes, L.; Cloutier, A.; Giuliano, M. Analysis of rheological and thermo-hygro-mechanical behaviour of stress-laminated timber bridge deck in variable environmental conditions Maderas. *Cienc. Tecnol.* **2012**, *14*, 303–319.
48. Åkerholm, M.; Hinterstoisser, B.; Salmén, L. Characterization of the crystalline structure of cellulose using static and dynamic FT-IR spectroscopy. *Carbohydr. Res.* **2004**, *339*, 569–578.
49. Nelson, M.L.; O'Connor, R.T. Relation of certain infrared bands to cellulose crystallinity and crystal lattice type. Part I. Spectra of lattice type I, II, III and of amorphous cellulose. *J. Appl. Polym. Sci.* **1964**, *8*, 1311–1324. [[CrossRef](#)]
50. Reiniati, I.; Osman, N.B.; McDonald, A.G.; Laborie, M.P. Linear viscoelasticity of hot-pressed hybrid poplar relates to densification and to the in situ molecular parameters of cellulose. *Ann. For. Sci.* **2015**, *72*, 693–703. [[CrossRef](#)]
51. FitzPatrick, M.A. Characterization and Processing of Lignocellulosic Biomass in Ionic Liquids. Ph.D. Thesis, Queen's University, Kingston, ON, Canada, 2011.
52. Široký, J.; Blackburn, R.S.; Bechtold, T.; Taylor, J.; White, P. Attenuated total reflectance Fourier-transform Infrared spectroscopy analysis of crystallinity changes in lyocell following continuous treatment with sodium hydroxide. *Cellulose* **2010**, *17*, 103–115.
53. Marson, G.A.; El Seoud, O.A. Cellulose dissolution in lithium chloride/*N,N*-dimethylacetamide solvent system: Relevance of kinetics of decrystallization to cellulose derivatization under homogeneous solution conditions. *J. Polym. Sci. Part A Polym. Chem.* **1999**, *37*, 3738–3744. [[CrossRef](#)]
54. ASTM International. *ASTM D143–94. Standard Test Methods for Small Clear Specimens of Timber*; ASTM International: West Conshohocken, PA, USA, 2007.

55. Bayani, S.; Baziyar, B.; Mirshokraie, S.A.; Taghiyari, H.R. Effects of heat treatment on the relative amounts of cellulose in nanosilver-impregnated and untreated poplar wood (*Populus alba*). *Floresta Ambiente* **2019**, *26*, e20160398. [[CrossRef](#)]
56. Fahlén, J.; Salmén, L. Cross-sectional structure of the secondary wall of wood fibers as affected by processing. *J. Mater. Sci.* **2003**, *38*, 119–126. [[CrossRef](#)]
57. Hakkou, M.; Pétrissans, M.; Zoulalian, A.; Gérardin, P. Investigation of wood wettability changes during heat treatment on the basis of chemical analysis. *Polym. Degrad. Stab.* **2005**, *89*, 1–5. [[CrossRef](#)]
58. Tjeerdsma, B.F.; Boonstra, M.; Pizzi, A.; Tekely, P.; Militz, H. Characterization of thermal modified wood: Molecular reasons for wood performance improvement. CPMA 13 CNMR characterization of thermally modified wood. *Holz Roh Werkst.* **1998**, *56*, 149–153. [[CrossRef](#)]
59. Tjeerdsma, B.F.; Militz, H. Chemical changes in hydrothermal treated wood: FTIR analysis of combined hydrothermal and dry heat-treated wood. *Holz Roh Werkst.* **2005**, *63*, 102–111. [[CrossRef](#)]
60. Esteves, B.; Graca, J.; Pereira, H. Extractive composition and summative chemical analysis of thermally treated eucalypt wood. *Holzforchung* **2008**, *62*, 344–351. [[CrossRef](#)]
61. Müller, G.; Schöpfer, C.; Vos, H.; Kharazipour, A.; Polle, A. FTIR-ATR spectroscopic analyses of changes in wood properties during particle- and fiberboard production of hard- and softwood trees. *BioResources* **2009**, *4*, 49–71.
62. Lionetto, F.; Del Sole, R.; Cannolett, D.; Vasapollo, G.; Maffezzoli, A. Monitoring wood degradation during weathering by cellulose crystallinity. *Materials* **2012**, *5*, 1910–1922. [[CrossRef](#)]
63. Borrega, M.; Kärenlampi, P.P. Hygroscopicity of Heat-Treated Norway Spruce (*Picea abies*) wood. *Eur. J. Wood Wood Prod.* **2010**, *68*, 233–235. [[CrossRef](#)]
64. Taghiyari, H.R. Effects of heat-treatment on permeability of untreated and nanosilver-impregnated native hardwoods. *Maderas Cienc. Tecnol.* **2013**, *15*, 183–194. [[CrossRef](#)]
65. Kato, K.L.; Cameron, R.E. Structure-property relationships in thermally aged cellulose fibers and paper. *J. Appl. Polym. Sci.* **1999**, *74*, 1465–1477. [[CrossRef](#)]
66. Matsuda, Y.; Isogai, A.; Onabe, F. Effects of thermal and hydrothermal treatments on the reswelling capabilities of pulps and paper sheets. *J. Pulp Paper Sci.* **1994**, *20*, 323–327.
67. Weise, U. Hornification: Mechanisms and terminology. *Paper Timber* **1998**, *80*, 110–115.
68. Taghiyari, H.R.; Moradi Malek, B. Effect of heat treatment on longitudinal gas and liquid permeability of circular and square-shaped native hardwood specimens. *Heat Mass Transf.* **2014**, *50*, 1125–1136. [[CrossRef](#)]
69. Hatakeyama, T.; Nakamura, K.; Hatakeyama, H. Studies on heat capacity of cellulose and lignin by differential scanning calorimetry. *Polymer* **1982**, *23*, 1801–1804. [[CrossRef](#)]
70. Phuong, L.X.; Shida, S.; Saito, Y. Effects of heat treatment on brittleness of *Styrax tonkinensis* wood. *J. Wood Sci.* **2007**, *53*, 181–186. [[CrossRef](#)]
71. Borrega, M. Mechanisms Affecting the Structure and Properties of Heat-Treated and High-Temperature Dried Norway Spruce (*Picea abies*) Wood. Ph.D. Thesis, School of Forest Sciences, University of Eastern Finland, Joensuu, Finland, 2011.
72. Cousins, W.J. Young's modulus of hemicelluloses as related to moisture content. *Wood Sci. Technol.* **1978**, *12*, 161–167. [[CrossRef](#)]
73. Irvine, G.M. The significance of the glass transition of lignin in thermomechanical pulping. *Wood Sci. Technol.* **1985**, *19*, 139–149. [[CrossRef](#)]

